Int J Thermophys (2010) 31:113–130
DOI 10.1007/s10765-010-0705-0

Real-Time Monitoring of Heat-Induced Aggregation of β-Lactoglobulin in Aqueous Solutions Using High-Resolution Ultrasonic Spectroscopy

Agnieszka Ochenduszko · Vitaly Buckin

Received: 5 May 2009 / Accepted: 16 January 2010 / Published online: 7 February 2010

Abstract High-resolution ultrasonic spectroscopy was applied for real-time monitoring of the heat-induced denaturation and aggregation processes in aqueous solutions of β-lactoglobulin. The temperature profiles for the ultrasonic velocity and attenuation in the frequency range from 4 MHz to 16 MHz were measured during heating and cooling cycles, 35 °C to 120 °C to 35 °C, with different heating and cooling rates. Two processes were identified in the heating profiles: transition to the molten globular state followed by formation of protein aggregates. Both processes are accompanied by a decrease in the ultrasonic velocity and an increase in compressibility. The ultrasonic attenuation did not show a significant change during the transition to the molten globule but increased significantly during aggregation. The diameter of the aggregates (calculated from ultrasonic attenuation) was of the order of 100 nm and depended on the pH and the heating rate. Variation of pH from 6.0 to 7.5 had a pronounced effect on the size of protein aggregates. Some effect of pH on the intrinsic properties of aggregates was also detected.

Keywords Aggregation · β-Lactoglobulin · Denaturation · High-resolution ultrasonic spectroscopy · Molten globule · Protein nano-particles · Ultrasonic attenuation · Ultrasonic velocity

1 Introduction

The functional behavior of proteins is strongly determined by their stable three-dimensional structure, which is maintained by hydrophobic interactions, hydrogen

A. Ochenduszko · V. Buckin (✉)
School of Chemistry and Chemical Biology, University College Dublin, Belfield, Dublin 4, Ireland
e-mail: vitaly.buckin@ucd.ie

bindings, electrostatic interactions, covalent bindings, and van der Waals forces. A significant number of protein applications require their thermal processing, which often alters their molecular structure and interactions, and can lead to aggregation. Some protein formulations (e.g., pharmaceuticals) are rigorously required to be aggregate-free to provide active and safe products; others are based on the functional properties of structures assembled during aggregation. For instance, a number of "heat-assembled" whey protein gels are utilized by the food industry for structuring products and controlling texture. The structural and physical properties of these gels are strongly influenced by the environmental and processing conditions during the aggregation process [1–9].

β-Lactoglobulin, the major whey protein in bovine milk, has often served as a model protein for studying heat-induced aggregation and gelation phenomena of globular proteins and has been widely investigated in the past [4,6–17]. At neutral pH and room temperature, native β-lactoglobulin exists as a stable noncovalent dimer [10,11]. At temperatures above room temperature, the β-lactoglobulin dimer dissociates to native monomers, which undergo conformational modifications [12]. These conformational changes involve exposure of both the interior hydrophobic residues and the sulfhydryl group that become available for intermolecular interactions (cross-links) [13,14]. Above approximately 65 °C, the protein exists in the state which was classified by several authors [12,15,16] as a molten globule state. Hydrophobic interactions between the exposed groups promote aggregation of the protein molecules while still in the molten-globule state. The exposed thiol group can induce thiol/disulfide exchange reactions, leading to the formation of disulfide-linked aggregates.

If the ionic strength is sufficiently low and at low pH, heat-induced aggregation proceeds relatively slowly and leads to the formation of transparent or translucent fine-stranded gels, composed of nanometer-thick networks [1,4–8]. Heat-induced aggregation is accelerated in screened conditions (pH around isoelectric point 5.1, increased ionic strength) and results in the formation of a white opaque particulate gel composed of aggregates which may reach micrometer size [4,7–9]. Bromley et al. [9] showed that the particle sizes of gels: (a) decrease with increasing heating rate and (b) decrease with increasing final temperature of incubation. Overall, the thermally induced aggregation of β-lactoglobulin is a multistage process, where each of the stages shows complex kinetics [17–19]. It was shown that the response of β-lactoglobulin to elevated temperatures depends on how the sample is heated [9,13,19]. The rate of aggregation is strongly affected by the temperature of incubation, heating rate, pH, ionic strength, and concentration of the protein [13,18,19]. The size of resulting aggregates depends highly on the environmental conditions and processing stresses employed. However, the exact relationship between the processing conditions and the structure and size of the aggregates are still not clear. An understanding of the details of complex kinetics of aggregation processes in different environmental conditions requires experimental techniques able to provide real-time information on assembly and growth of protein aggregates as well as on the changes in their structure during all stages of thermally induced processes. A number of different analytical techniques, such as electron microscopy, atomic force microscopy, light scattering, differential scattering calorimetry (DSC), nuclear magnetic resonance (NMR), circular dichroism, electrophoresis, chromatography, rheometry, etc.

has been employed in the past in the analysis of protein aggregation [4,9,12,16,20]. However, real-time assessment of the formation of protein aggregates and nano-assemblies is a difficult task for traditional analytical techniques, especially when information on both the size and the intrinsic properties of the aggregates is required in a broad range of temperatures and states (solution, suspension of protein nano-particles, and gel).

Our paper reports the results of the application of high-resolution ultrasonic spectroscopy for real-time monitoring of aggregation processes in aqueous solutions of β-lactoglobulin. This technique is nondestructive, capable of rapid and precise measurements, requires no sample preparation and no markers, can be applied to systems that are optically opaque, and allows measurements in a broad range of temperatures and concentrations including those relevant to industrial protein processing [21,22]. This technique provides information on the two levels of organization of protein systems: intrinsic properties of protein globules and protein particles and the size of protein aggregates. Previously, ultrasonic spectroscopy has been applied to study proton transfer, hydration, and phase transitions in proteins systems [23–27]. Most previous applications of ultrasonic spectroscopy in protein systems utilized ultrasonic devices based on the pulse technique. These instruments have a broad frequency range; however, the resolution in ultrasonic velocity was limited, about $0.1\ \mathrm{m \cdot s^{-1}}$, which does not allow resolving details of the thermally induced microstructural changes of intrinsic properties of protein globules and protein particles. Another limitation of this spectroscopy is the requirement of relatively large sample volumes, which complicates measurements in the temperature ramp regime. Measurements of the ultrasonic velocity at one frequency provided much better resolution (down to $1\ \mathrm{mm \cdot s^{-1}}$) in small sample volumes and have been successfully used for analysis of the compressibility of proteins in solutions [28–35]. However, the absence of data for the ultrasonic velocity and attenuation in a broad frequency range did not allow analysis of scattering effects. In addition, most of these devices had also limited operating temperature and pressure ranges (elevated pressures are required to avoid boiling of aqueous solutions at temperatures above 100 °C). High-resolution ultrasonic spectrometers provide excellent resolution for both velocity (down to $0.2\ \mathrm{mm \cdot s^{-1}}$) and attenuation (down to 0.2 %) [21,22], cover the frequency range from 1 MHz to 20 MHz and allow measurements at elevated pressures and in a broad temperature range (−40 °C to 130 °C) in isothermal and temperature ramp regimes, which cover most processing conditions of protein formulations. The technique has been successfully applied in the ultrasonic analysis of heat-induced coagulation in milks [36,37], monitoring of acid gelation processes [38] and rennet induced gelation in milk [39], and denaturation of whey proteins [27] and other systems. In the present study we have used high-resolution ultrasonic spectroscopy for real-time assessment of structural transformations and aggregation of β-lactoglobulin at different heating rates and pH in the temperature range from 35 °C to 120 °C. The ultrasonic velocity provided information on evolution of the compressibility ("rigidity") of protein globules and protein aggregates and attenuation on the growing size of protein aggregates. Detailed interpretation of the experimental results requires a comprehensive multivariant analysis of the ultrasonic velocity and attenuation as a function of frequency, pH, concentration, heating speed, etc., and will be a subject of future studies. However, presented in this paper, a qualitative study provides

new information on real-time analysis of the key processes (denaturation, aggregation, and gelation) which occur in aqueous solutions of β-lactoglobulin during continuous heating.

2 Measurements

2.1 Materials

β-lactoglobulin (L3908) was purchased from Sigma-Aldrich (Dublin, Ireland). Protein samples were dissolved in 0.1 M NaCl (Sigma Aldrich, S-7653) and then stirred at room temperature for 1 h. The pH of protein solutions was adjusted to the required value in the range between 6 and 7.5 by adding small amounts of 0.1 M hydrochloric acid (Sigma Aldrich, 31, 894-9) or sodium hydroxide (Sigma Aldrich, 31, 951-1). The concentration of β-lactoglobulin was determined spectrophotometrically at 278 nm using the extinction coefficient $\varepsilon_{278} = 0.955\,\mathrm{cm}^2 \cdot \mathrm{mg}^{-1}$ [40]. All solutions were deeply degassed prior to measurements.

2.2 Procedures

2.2.1 High-Resolution Ultrasonic Spectroscopy

The temperature profiles of the ultrasonic velocity, u, and attenuation, α, were measured at several selected frequencies in a range from 4 MHz to 16 MHz using an HR-US 102 ultrasonic spectrometer (Ultrasonic Scientific Ltd.) in the temperature ramp regime. This device is equipped with two cells enabling single-cell or differential measurements. The differential regime allows resolution of $0.2\,\mathrm{mm} \cdot \mathrm{s}^{-1}$ for the ultrasonic velocity and 0.2 % for the ultrasonic attenuation. The temperature was controlled with a Haake F8 heating bath, which provided a temperature stability of 0.01 °C. The temperature was recorded by the sensor embedded in the body of the differential ultrasonic cell as provided by the manufacturer. The temperature readings were verified by measuring the ultrasonic velocity in pure water for which the temperature dependence is well known [41], using the same temperature ramp procedures as for protein solutions. We did not see a significant difference in the temperature profiles of the velocity in pure water at different ramp speeds utilized in our measurements ($0.02\,^\circ\mathrm{C} \cdot \mathrm{min}^{-1}$ to $1\,^\circ\mathrm{C} \cdot \mathrm{min}^{-1}$). This showed an absence of a noticeable gradient of temperature within our 1 mL samples in the cells during the temperature ramps, which could affect our data for proteins, especially because the observed transitions are relatively broad on the temperature scale (few degrees).

2.2.1.1. Measuring Procedure 1.1 mL of freshly prepared and deeply degassed solution of β-lactoglobulin was loaded into the measuring cell of the HR-US 102 spectrometer, set at 35 °C. The same volume of deionized water was loaded into the reference cell. Solutions were left for 10 min to equilibrate, and measurements of the ultrasonic velocity and attenuation at selected frequencies (4.7 MHz, 5.1 MHz, 7.4 MHz, and 15.6 MHz) were activated and continuously measured for 10 min. Then, the tempera-

ture ramp with a preset ramp speed was activated during which the ultrasonic velocity and attenuation were continuously measured at the above preselected frequencies. The typical ramp parameters were 35 °C to 120 °C at a constant rate, 0.01 °C · min^{-1} to 1 °C · min^{-1} (in different ramps). Some of the ramps were programmed to include a downscan to 35 °C after reaching 120 °C. Screw caps fitted with a septum were used to maintain pressure inside the cell and avoid boiling. Ultrasonic temperature profiles were measured in, at least, duplicates. The typical reproducibility of the temperature profiles was within the limits of scatter of the data points presented in the figures.

2.2.1.2 Baseline Subtraction The same temperature ramps as described above were performed separately for the solvent (0.1 M NaCl), which then were subsequently subtracted from the ultrasonic velocity and attenuation profiles measured in protein samples. Therefore, the data shown below (all figures for attenuation and the insert in Fig. 2 for velocity), represent the change of the excess attenuation and velocity (the contribution to ultrasonic attenuation and velocity caused by the addition of protein to the solvent) with temperature.

2.2.2 Ultrasonic Particle Sizing

Calculations of the average particle size as well as expected scattering contributions to the ultrasonic velocity and attenuation were carried out using the particle size module "Psize289", provided with the HR-US 102 spectrometer. This software utilizes multiple scattering theories described earlier (see, for example, [42–44]). It allows calculation of the dependence of the ultrasonic velocity and attenuation on the size of particles (Fig. 4) as well as calculations of the average particle size from the measured value of the ultrasonic attenuation and the thermophysical parameters of the continuous and dispersed phases.

The following parameters for dispersed and continuous phases were used in the calculations:

(1) *Dispersed phase*: density, ρ(1325 kg · m^{-3} at 80 °C and 1322 kg · m^{-3} at 90 °C); specific heat capacity, C_p(2271 J · kg^{-1} · K^{-1} at 80 °C and 2274 J · kg^{-1} · K^{-1} at 90 °C); thermal conductivity, γ(0.2669 W · m^{-1} · K^{-1} at 80 °C and 0.2744 W · m^{-1} · K^{-1} at 90 °C), ultrasonic velocity, u(1121 m · s^{-1}); thermal expansion coefficient, β(3.5 × 10^{-4} K^{-1} at 80 °C and 2.6 × 10^{-4} K^{-1} at 90 °C), and attenuation per square of frequency, αf^{-2}(3 × 10^{-12}m^{-1} · Hz^{-2}). The density of β-lactoglobulin up to 90 °C was taken as the inverse of its apparent specific volume, measured by us using Anton Paar DMA 5000 density meter. The values of the thermal conductivity at 80 °C and 90 °C were obtained from the thermal conductivity model (dependence of thermal conductivity on temperature) of whey proteins [45], and the specific heat capacity at 80 °C and 90 °C was estimated from the specific-heat-capacity model of protein [45]. The thermal expansion coefficient for protein was calculated from our data on the temperature dependence of the apparent volume of β-lactoglobulin, and the ultrasonic velocity in protein was calculated from the density of protein and the coefficient of adiabatic compressibility β_M = 60 × 10^{-6} bar^{-1} at 25 °C (see discussion

below, [31]). Although at 80 °C and 90 °C, this value is supposed to be slightly higher, its effect on particle size has not been significant for our estimations. Ultrasonic attenuation in protein was taken from [37]; because we analyze only the changes in ultrasonic attenuation caused by scattering effects, the absolute values of attenuation in continuous phase and in the protein do not significantly affect our calculations.

(2) *Continuous phase* (0.1 M NaCl): density, ρ(975.64 $kg \cdot m^{-3}$ at 80 °C and 969.10 $kg \cdot m^{-3}$ at 90 °C; calculated from data for aqueous solutions of NaCl [46]); specific heat capacity, C_p(4159.3 $J \cdot kg^{-1} \cdot K^{-1}$ at 80 °C and 4166.98 $J \cdot kg^{-1} \cdot K^{-1}$ at 90 °C; obtained by extrapolation of data presented in [47,48] to concentration of 0.1 M NaCl and required temperatures); thermal conductivity, γ(0.669 $W \cdot m^{-1} \cdot K^{-1}$ at 80 °C and 0.675 $W \cdot m^{-1} \cdot K^{-1}$ at 90 °C [49]), ultrasonic velocity, u(1559.28 $m \cdot s^{-1}$ at 80 °C and 1555.25 $m \cdot s^{-1}$ at 90 °C [50]); thermal expansion coefficient, β(6.32×10^{-4} K^{-1} at 80 °C and 6.88×10^{-4} K^{-1} at 90 °C; calculated from data on the temperature dependence of the apparent volume [46]), and attenuation per square of frequency, αf^{-2} (as measured, 8×10^{-15} $m^{-1} \cdot Hz^{-2}$ at 80 °C and 7.3×10^{-15} $m^{-1} \cdot Hz^{-2}$ at 90 °C).

2.2.3 Photon Correlation Spectroscopy

The average diameter of protein particles was measured at preset temperatures between 35 °C and 90 °C with Zetasizer Nano ZS, Malvern Instruments at an angle of 173 °. The temperature was controlled within 0.1 °C with a Peltier temperature controller. The thermal cap (provided with the instrument) was used to ensure temperature stability during the measurements.

Protein samples were prepared in the same way as for ultrasonic measurements. The samples were filtered prior to measurement using 0.02 μm sterile inorganic membrane filters (Anatop 10, Whatman, Cat. No. 68091102).

3 Results

3.1 Temperature Profiles of Ultrasonic Velocity and Attenuation

Figure 1 shows the temperature profile of ultrasonic attenuation in 2 % w/w β-lactoglobulin aqueous solution at pH 7.5 upon heating and cooling (35 °C to 120 °C to 35 °C) ramps at 0.2 $°C \cdot min^{-1}$. The attenuation value at 35 °C was subtracted to illustrate the change in attenuation caused by protein aggregation. Only the results for the interval from 60 °C to 90 °C is presented as other temperature intervals do not possess any new features. Three stages in the heating temperature profile of ultrasonic attenuation can be seen. (1) No changes in the excess ultrasonic attenuation were observed at heating up to 66 °C. (2) A sharp increase in attenuation was found between 68 °C and 76 °C (approximately), with the higher magnitude at higher frequencies. This increase in attenuation can be attributed to the scattering of ultrasonic waves on protein aggregates formed as a result of protein denaturation. (3) Above 76 °C, attenuation levels off (small increase in

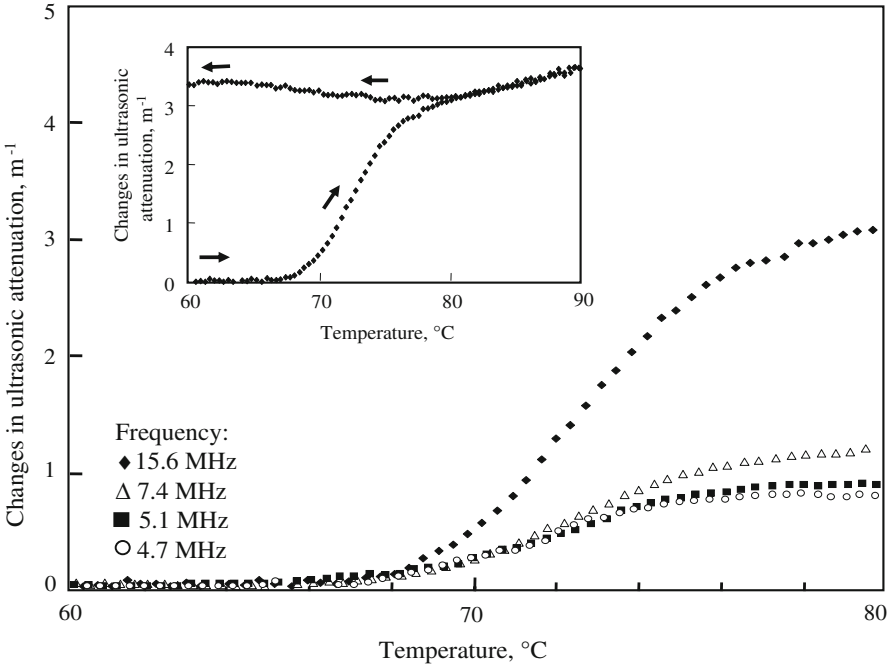

Fig. 1 Changes in ultrasonic attenuation (solvent baseline subtracted as described in the text) during continuous heating from 35 °C to 120 °C (ramp speed of 0.2 °C · min^{-1}) of 2 % w/w β-lactoglobulin aqueous solution containing 0.1 M NaCl at pH 7.5, measured at 4.7 MHz, ◯, 5.1 MHz, ■, 7.4 MHz, Δ, and 15.6 MHz, ♦. Attenuation at 35 °C was subtracted from the temperature profiles. Only the 60 °C to 80 °C interval is presented as other temperature intervals do not possess any new features. Inset shows the attenuation profile at 15.6 MHz obtained during heating and subsequent cooling of the β-lactoglobulin sample

attenuation was observed at 15.6 MHz). The inset in Fig. 1 shows the attenuation profile upon heating to 120 °C and subsequent cooling at 15.6 MHz. The reversibility of the temperature profile was observed for the stage (3) only. At other stages the attenuation value did not recover in the cooling cycle, and at 35 °C, was about 3.4 m^{-1} higher that the initial value. This could be interpreted by the scattering effects from the residual protein aggregates, which do not dissolve upon cooling.

Figure 2, inset (a), shows change in the ultrasonic velocity in 2 % w/w β-lactoglobulin aqueous solution at pH 7.5 upon heating at 0.2 °C · min^{-1} from 35 °C to 120 °C at 15.6 MHz. A gradual decrease in velocity was observed up to 50 °C followed by a drop in velocity at higher temperatures. This linear part of the curve was extrapolated to higher temperatures and subtracted from the temperature profile of the ultrasonic velocity, and results (excess ultrasonic velocity) are shown in the main frame of Fig. 2. This procedure eliminates the heat expansion effects (increase in volume and compressibility of the protein with temperature) from the temperature profile and provides a better representation of the effects of heat transitions, which occur at temperatures above 50 °C, on the ultrasonic velocity. Several stages can be distinguished in the velocity profile. (1) No changes in the excess ultrasonic velocity were observed up to 50 °C. (2) At 50 °C the velocity started to decrease. This decrease

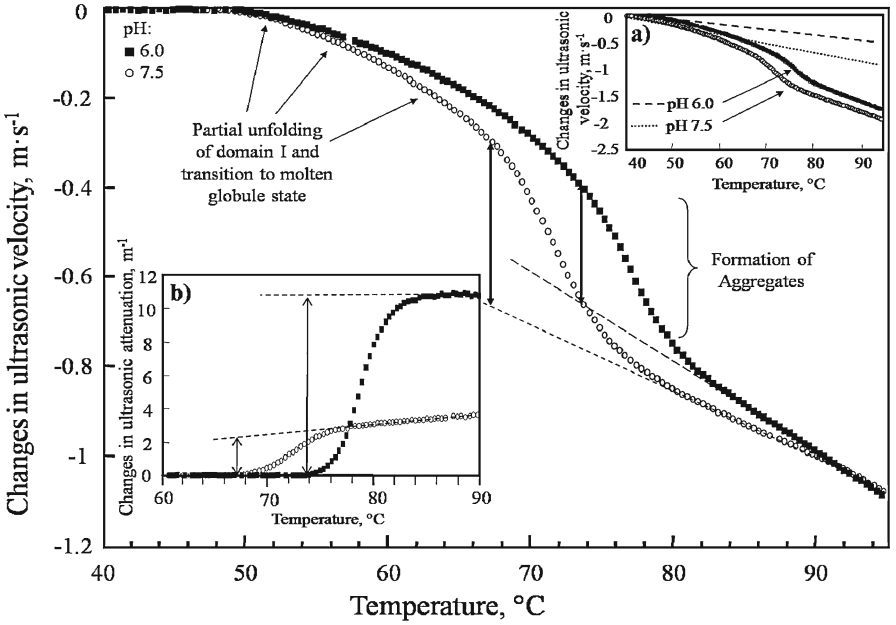

Fig. 2 Changes in ultrasonic velocity at 15.6 MHz during continuous heating from 40 °C to 120 °C (ramp speed of 0.2 °C · min^{-1}) of 2 % w/w β-lactoglobulin aqueous solution containing 0.1 M NaCl at pH 6.0, ■, and 7.5, ◯. The solvent baseline and linear extrapolation of the initial part of the curve (35 °C to 50 °C, see inset a) were subtracted as described in the text. Only the 40 °C to 95 °C interval is presented as other temperature intervals do not possess any new features. Inset *a* shows changes in ultrasonic velocity in an aqueous solution of β-lactoglobulin at pH 6.0 and 7.5 and extrapolation of initial parts of the curves for both values of pH (solvent baseline subtracted as described in the text). Inset *b* shows the ultrasonic attenuation profile (solvent baseline subtracted) between 60 °C and 90 °C at 15.6 MHz in β-lactoglobulin solutions at pH 6.0 and 7.5

can be related to the partial unfolding of the protein and transition to the liquid-like "molten globule" state, which is expected to occur above 50 °C [12,15,16]. (3) A sharp drop in the excess ultrasonic velocity is seen between 67 °C and 76 °C (approximately) for pH 7.5 and between 74 °C and 82 °C (approximately) for pH 6.0. This major change in ultrasonic velocity coincided with the increase in the ultrasonic attenuation and can be attributed to the formation and growth of the highly compressible protein aggregates. (4) Above 76 °C at pH 7.5 and above 82 °C at pH 6.0, the velocity gradually decreased with temperature. This can be related to the temperature characteristic (increase of volume and compressibility with temperature) of the protein aggregate formed at the second stage of the process. A small frequency dependence of the temperature profiles of ultrasonic velocity was observed at temperatures above 70 °C, indicating a significant size of protein aggregates (see below).

3.2 Effect of pH and the Heating Rate on the Temperature Profiles of the Ultrasonic Velocity and Attenuation

Figure 2, main frame and inset (b), show the temperature profiles for the ultrasonic velocity and attenuation in 2 % w/w β-lactoglobulin aqueous solution at pH 7.5 and

Table 1 Effect of protein aggregation on ultrasonic velocity, Δu, and attenuation, $\Delta\alpha$, in 2% aqueous (0.1 M NaCl) solution of β-lactoglobulin at 15.6 MHz

pH	T^{a} (°C)	Δu^{b} ($m \cdot s^{-1}$)	$\Delta\alpha^{c}$ (m^{-1})
6.0	73.8	−0.27	10.7
7.5	67.2	−0.36	2.25

[a] Temperature of the beginning of aggregation determined from the attenuation curves
[b] Difference between the ultrasonic velocity measured at the temperature of the beginning of the aggregation and the linear extrapolation of the post-aggregation profile to the same temperature (see Fig. 2)
[c] Difference in ultrasonic attenuation measured at the temperature of the beginning of the aggregation and the linear extrapolation of the post-aggregation profile to the same temperature

6.0 upon heating at $0.2\,°C \cdot min^{-1}$. Table 1 summarizes the aggregation effect on the ultrasonic velocity and attenuation recorded at both values of pH and a frequency of 15.6 MHz. The values revealed in Table 1 summarise the differences between ultrasonic parameters measured at the temperature at the beginning of the aggregation and extrapolated (linear) to the same temperature post-aggregation profile. The temperature of the beginning of aggregation was determined from the attenuation curve. Figure 3, the main frame and the inset, shows the changes in the ultrasonic velocity and attenuation at 15.6 MHz in 2% w/w β-lactoglobulin aqueous solution at pH 6.8 upon heating at (0.02, 0.1, and 1) $°C \cdot min^{-1}$ from 35 °C to 120 °C.

4 Discussion

4.1 Ultrasonic Velocity

In low attenuating liquids, the ultrasonic velocity, u, is determined by the density, ρ, and the coefficient of adiabatic compressibility, β, of the medium [51]:

$$u = (\beta\rho)^{-\frac{1}{2}}. \tag{1}$$

The compressibility parameter is particularly important, as the elastic response of the sample to compressions and decompressions in ultrasonic waves is extremely sensitive to intermolecular interactions and molecular organization.

The contribution of a solute to the ultrasonic velocity can be characterized through the concentration increment of the ultrasonic velocity, a, defined by

$$a = \frac{u - u_0}{u_0 c}, \tag{2}$$

where u and u_0 are the ultrasonic velocities of the solution and solvent, respectively, and c is the concentration of solute (g per cm^3 of solution in this paper).

Heat-induced aggregation of proteins at our concentrations often results in formation of protein particle gel where cross-linked protein particles form a

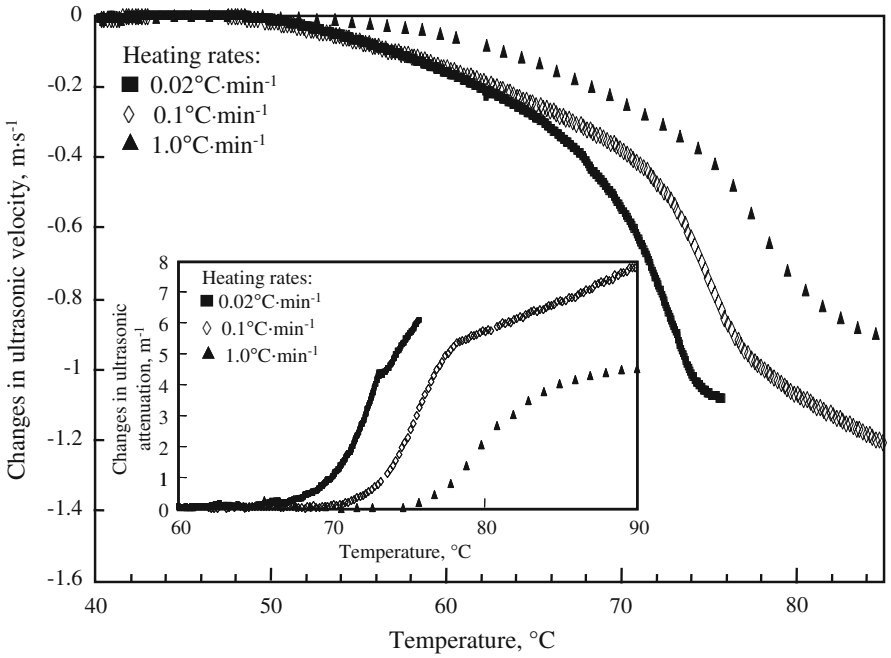

Fig. 3 Changes in the ultrasonic velocity (solvent baseline and second baseline, linear extrapolation of the initial part of the curve, were subtracted as is shown in Fig. 2, inset *a*) at 15.6 MHz during continuous heating from 40 °C to 120 °C of 2 % w/w β-lactoglobulin aqueous solution containing 0.1 M NaCl at pH 6.8 at heating rates: 0.02 °C · min^{-1}, ■, 0.1 °C · min^{-1}, ◇, and 1 °C · min^{-1}, ▲. Only the 40 °C to 85 °C interval is presented as other temperature intervals do not possess any new features. Inset shows changes in ultrasonic attenuation (solvent baseline subtracted) recorded at 15.6 MHz during continuous heating from 40 °C to 120 °C of 2 % w/w β-lactoglobulin at heating rates of 0.02 °C · min^{-1}, ■, 0.1 °C · min^{-1}, ◇, and 1 °C · min^{-1}, ▲. Only the 60 °C to 90 °C interval is presented

three-dimensional network. This produces a decrease of the compressibility of the sample due to the added rigidity of the gel network. The contribution of protein gels to the ultrasonic velocity was analyzed earlier for acid casein gels [38] and rennet-induced gels [39] and it was found that it does not exceed 0.1 m · s^{-1} at 15 MHz at concentration of proteins close to the concentration of our samples, which is smaller and of opposite sign than the observed changes in the velocity caused by denaturation and aggregation in our samples. Therefore, this contribution could be neglected in further qualitative discussion.

In dilute solutions, the concentration increment of ultrasonic velocity is related to the physical characteristics of the solute and solvent by the following equation [52]:

$$a \cong \varphi V - \frac{\varphi K_S}{2\beta_{S_0}} - \frac{1}{2\rho_0}, \tag{3}$$

where φV ($\equiv \frac{V-V_0}{m}$; $(V - V_0)$ is the apparent volume of the solute and is the change of volume (cm^3) caused by the addition of mass m (g) of solute to the volume V_0 of a pure solvent) and φK_s ($\equiv \frac{K-K_0}{m}$; $K \equiv -\left(\frac{\partial V}{\partial P}\right)_S$; $K_0 \equiv -\left(\frac{\partial V_0}{\partial P}\right)_S$) is the apparent

adiabatic compressibility of the solute ($\mathrm{cm}^3 \cdot \mathrm{g}^{-1} \cdot \mathrm{bar}^{-1}$); $\beta_{S_0} (\equiv -\frac{1}{V_0}\left(\frac{\partial V_0}{\partial P}\right)_s)$ is the coefficient of adiabatic compressibility of pure solvent, and ρ_0 is the density of pure solvent. Equation 3 is a consequence of Eqs. 1 and 2 and the definitions of φV and φK_S.

Our measurements of the temperature profiles of the density in our samples (data not shown) indicated that the changes in apparent volume accompanying heat-induced protein denaturation in our systems are small and their contribution constitutes less than 10 % of overall experimentally observed changes in ultrasonic velocity. This is in agreement with the previous observations for protein denaturation and transition to a molten globular state [29,53,63]. Therefore, the changes in the concentration increment of ultrasonic velocity accompanying the heat-induced transitions of protein shall be attributed mainly to the changes of the apparent adiabatic compressibility of proteins:

$$\Delta a \cong -\frac{\Delta \varphi K_S}{2\beta_{S_0}}. \tag{4}$$

Formation of protein particles, as a result of aggregation, produces an additional, "scattering," contribution to the ultrasonic velocity, caused by thermal and visco-inertial scattering effects. Because the density of proteins is close to the density of water (20 % difference), the visco-inertial contribution shall be small and can be neglected [44,54]. The thermal "scattering" contribution results in a decrease of the apparent adiabatic compressibility with an increase of the size of aggregates caused by a reduction of the amount of solvent involved in the solute–solvent heat exchange when the solutes aggregate [54]. In this work, we have used the particle size module provided with the HR-US 102 spectrometer to estimate the change of ultrasonic velocity caused by formation of protein aggregates of the size corresponding to the measured change of attenuation (see below). The calculated increase in the ultrasonic velocity is about $0.2\,\mathrm{m} \cdot \mathrm{s}^{-1}$ for pH 6.0, which is comparable with but of the opposite sign than the absolute value of the observed decrease in the ultrasonic velocity caused by protein denaturation and aggregation ($-0.27\,\mathrm{m} \cdot \mathrm{s}^{-1}$). At pH 7.5, this increase is smaller, $0.1\,\mathrm{m} \cdot \mathrm{s}^{-1}$. Therefore we can assume that the main contribution to the observed changes in the ultrasonic velocity (and compressibility) caused by protein denaturation and aggregation comes from the intrinsic properties of protein and its hydration.

When the scattering contribution is subtracted, the apparent adiabatic compressibility of a solute can be represented by the sum of ideal, intrinsic, and hydration terms (see for discussion [33,52]:

$$\varphi K_S = k_{\mathrm{id}} + k_{\mathrm{M}} + \Delta k_{\mathrm{h}}, \tag{5}$$

where k_{id} is the "ideal" contribution of the solutes to the compressibility of the solution, k_{M} is the intrinsic compressibility of the solute molecule, and Δk_{h} is the hydration (solvation for nonaqueous solutions) contribution to the compressibility caused by a change in the compressibility of water (solvent) as a result of solute–solvent interactions and the compressibility of the void space between the solute molecule and surrounding molecules of the solvent. In some publication, the term Δk_{h} is split

into subterms [29,33,52]. The term k_{id} $\left(\equiv -\left(\frac{\partial v_{\mathrm{id}}}{\partial P}\right)_S\right)$ is the compressibility of the "ideal" contribution to the volume, v_{id}, which represents the increase of the volume of the liquid caused by solubilization of a solute with a negligibly small intrinsic volume in an ideal solution (no solute–solvent interactions). It results from the thermal motion of the solute molecules and can also be interpreted as an expansion of the solvent caused by the osmotic pressure of the solute. For high-molar mass compounds, this value is small compared with the other contributions to φK_S and can be neglected for our discussion. Both compressibilities, k_{M} and Δk_{h}, are not adiabatic because of the heat exchange between the protein molecules, their hydration shell, and the surrounding solution during the time of the compression cycle in the ultrasonic wave. The exact relationship between these values and the thermodynamic properties of the solute and the solvent was discussed previously [54]. However, because these values are of the same order as corresponding adiabatic and isothermal compressibilities, for qualitative discussion, we will not make this distinction.

An additional relaxation contribution to the apparent adiabatic compressibility may exist if the solute molecules have different conformational, protonated, tautomeric, or other states, which have a different apparent volume or enthalpy and for which the distribution can be affected changing the pressure and temperature in the ultrasonic wave [55]. The main contributor to the relaxation compressibility in solutions of proteins is the reaction of proton transfer, which is accompanied by substantial volume effects. Changes of pressure in ultrasonic waves shift the equilibrium between the protonated and deprotonated forms of amino acid residues, which results in a change of volume and therefore contributes to the compressibility. However, this contribution is substantial only at a pH below 4 and above 11 [56–61]. At a pH close to neutral, the relaxation contribution to the apparent adiabatic compressibility, φK_S, of globular proteins, is small and can be neglected [56].

Therefore, the apparent adiabatic compressibility of globular proteins is determined by a positive contribution of the protein interior, k_{M}, and the contribution due to hydration, Δk_{h}. The last contribution is normally negative because the hydration water is less compressible than the bulk water. This is a result of a high "structural" contribution to the compressibility of pure water, associated with the unique structure of pure water, representing a network of hydrogen bonds. This structure changes under applied pressure which results in a volume decrease. Hydration of hydrophilic atomic groups of solutes distorts this structure and therefore reduces the compressibility of water (see [52] for more discussion). The more rigid is the interior of the globular protein, the smaller is its intrinsic compressibility and, consequently, the smaller is the total partial compressibility of the protein. Also, the higher is the level of hydration (the more atomic groups of the protein are exposed to contact with water), the more negative is the hydration contribution to the apparent adiabatic compressibility and the smaller is its value.

4.2 Ultrasonic Attenuation

In homogeneous samples, the attenuation is determined by intrinsic properties of the medium. In heterogeneous samples, there is an additional scattering contribution to

ultrasonic attenuation, which is a function of particle size. The overall attenuation in suspensions can be expressed as

$$\alpha = \alpha_0 + \alpha_{\text{scattering}}, \tag{6}$$

where α_0 is the intrinsic attenuation due to the attenuation by continuous and dispersed (particles) media, and $\alpha_{\text{scattering}}$ is the attenuation due to the scattering of ultrasonic waves by colloidal particles. (Relaxation processes in solutions can also contribute to ultrasonic attenuation; however, in our pH range for the reasons discussed above, we will neglect this contribution.) The basic mechanism of the interaction of ultrasonic waves with solute particles in dispersions contains two major contributors, thermoelastic and visco-inertial scattering [42–44,62]. Thermoelastic scattering results from oscillations of temperature caused by adiabatic compressions and decompressions in ultrasonic waves. These oscillations in temperature create a heat flow between the particles and the surroundings. This flow heats and cools the boundary layer between the particles and the surroundings with an associated expansion and contraction of the boundary layer, thus turning the particles into a secondary source of ultrasonic waves. In addition, a thermal wave will flow away from the particles and attenuate. The source of visco-inertial scattering lies in the difference in density between the scatterer and its surroundings. The oscillating forces associated with the deformation in the ultrasonic wave result in a motion of particles relative to their surroundings. This motion increases with the increasing density difference between the particles and the surrounding fluid. The relative motion is a source of new waves and a shear field propagating away from the border between the particles and surrounding fluid, which attenuates away over a distance. The details of scattering theories and their application have been thoroughly discussed (see [44] as an example).

Figure 4 shows the change in the ultrasonic velocity and attenuation caused by an increase of the size of protein particles at a constant protein concentration for a frequency of 15.6 MHz, calculated at 80 °C using the particle size software module of an HR-US 102 spectrometer, and the physical properties of the solvent and solutes described above. These profiles were used for estimation of the size of aggregates formed and for prediction of the scattering effects of the ultrasonic velocity.

4.3 Interpretation of Temperature Profiles of Ultrasonic Velocity and Attenuation in Aqueous Solutions of β-Lactoglobulin

4.3.1 Partial Unfolding and Transition to "Molten Globule" State

As discussed above, the beginning of the heat transition in β-lactoglobulin is marked by a decrease in the excess ultrasonic velocity at 50 °C, which is not accompanied by any significant changes in ultrasonic attenuation. It was previously reported that at approximately 50 °C β-lactoglobulin undergoes conformational modifications, loses some elements of the tertiary and secondary structures, and partially unfolds [12,15,16]. At temperatures around and above 65 °C, β-lactoglobulin was described as being in a "molten globule state" [12,15,16], defined as a compact state with native-like

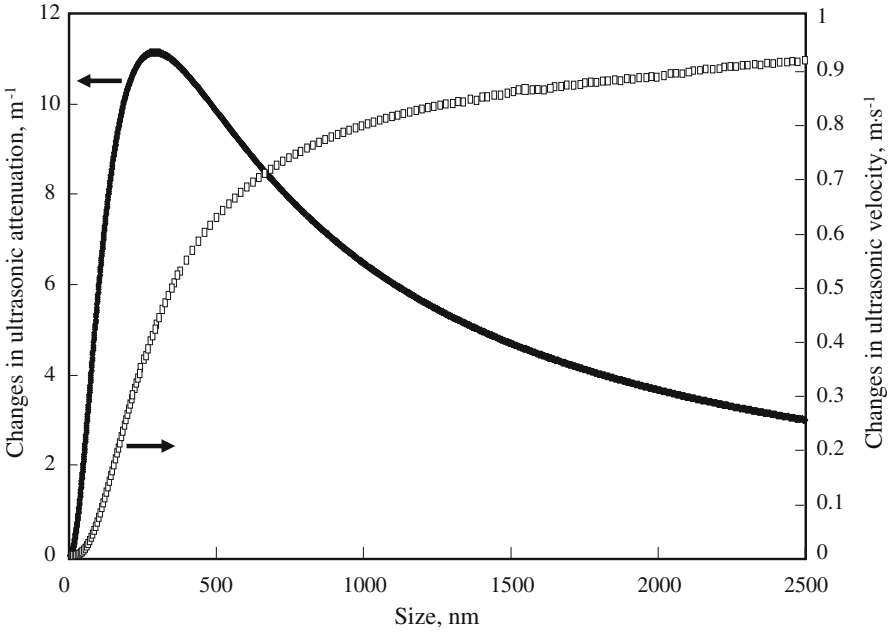

Fig. 4 Illustration of typical changes in ultrasonic velocity, □, and attenuation, ■, at 15.6 MHz caused by an increase of the size of protein particles at protein concentration 2 % calculated at 80 °C using the particle size software module "Psize289" of an HR-US 102 spectrometer. The attenuation and velocity at a size equal to zero were subtracted from the profile

secondary structure, having loosely packed and mobile side chains and a highly hydrated interior. From the changes in the ultrasonic velocity in a solution of β-lactoglobulin at pH 7.5 and 65 °C, we estimated the change in the concentration increment of the ultrasonic velocity upon transition to a molten globule, Δa, is about $-0.008\,\mathrm{cm^3 \cdot g^{-1}}$. By assuming that the major contribution to the change of the concentration increment of the ultrasonic velocity comes from the apparent adiabatic compressibility, we calculated that the change in the apparent adiabatic compressibility at the transition to the molten globule stage, $\Delta\varphi K_S$, is about $0.7 \times 10^{-6}\,\mathrm{bar^{-1} \cdot cm^3 \cdot g^{-1}}$. This is in line with previously reported changes in the apparent adiabatic compressibility of protein accompanying an acid- and pressure- induced transition to a molten globule, which are in the range of $(0.3 \times 10^{-6}$ to $4 \times 10^{-6})\,\mathrm{bar^{-1} \cdot cm^3 \cdot g^{-1}}$ for different protein systems [30,31,35,63–65]. The apparent adiabatic compressibility, φK_S, of native β-lactoglobulin at neutral pH is about $4.6 \times 10^{-6}\,\mathrm{bar^{-1} \cdot cm^3 \cdot g^{-1}}$ [34]. The observed change in the apparent adiabatic compressibility between 50 °C and 65 °C represents only about 15 % of this value.

The intrinsic compressibility of a protein globule, k_M, was previously estimated as about $(7 \text{ to } 23) \times 10^{-6}\,\mathrm{bar^{-1} \cdot cm^3 \cdot g^{-1}}$ and the coefficient of intrinsic compressibility, $\beta_M (\equiv k_M/\nu_M$, ν_M is the specific intrinsic volume of protein globule) was reported to be within the range of $(10 \text{ to } 23) \times 10^{-6}\,\mathrm{bar^{-1}}$ [34,35] at 25 °C. This value, β_M, is approximately 60 % less than the coefficient of the adiabatic compressibility of pure water

($45 \times 10^{-6}\,\mathrm{bar}^{-1}$). The value of β_M for β-lactoglobulin in the native state corresponds to the compressibility of a rigid, tightly packed, solid-like substance [33,35]. As there is no indication that this value would be significantly different at 65 °C, we can use it as a reference point in our discussion. If the observed change in the apparent compressibility is attributed to a change in the intrinsic compressibility of protein, β_M, only, it will produce the increase in the coefficient of compressibility, $\Delta\beta_M = \Delta\varphi K_S/v_M$, about $1 \times 10^{-6}\mathrm{bar}^{-1}$ (v_M for protein is about $0.75\,\mathrm{cm}^3 \cdot \mathrm{g}^{-1}$, see, for example, [33]), which is only a small portion (5 %) of the intrinsic compressibility of a protein globule. However, it is believed that the measured change in the apparent compressibility upon transition to a molten globule, $\Delta\varphi K_S$, is a sum of two values, the change of intrinsic and hydration contributions to the compressibility, which have opposite signs and are much larger by absolute value than $\Delta\varphi K_S$. Kharakoz and Bychkova [30] found that an acid-induced transition of native α-lactalbumin to a molten globule changed the apparent adiabatic compressibility by about $1.8 \times 10^{-6}\,\mathrm{bar}^{-1} \cdot \mathrm{cm}^3 \cdot \mathrm{g}^{-1}$, but the intrinsic compressibility coefficient changed by a factor of two, from $13 \times 10^{-6}\,\mathrm{bar}^{-1}$ for this native protein to $27 \times 10^{-6}\,\mathrm{bar}^{-1}$ for a molten globule. This was explained by a significant increase in hydration of the interior of α-lactalbumin during the native-to-molten globule state transition, which lowers the compressibility of water, and therefore compensates the increase in the apparent compressibility caused by the "softening" of the protein globule. Chalikian et al. [31] showed that the acid-induced transition of native cytochrome c to a molten globule resulted in an increase in the apparent adiabatic compressibility by $3.8 \times 10^{-6}\,\mathrm{bar}^{-1} \cdot \mathrm{cm}^3 \cdot \mathrm{g}^{-1}$. They calculated the intrinsic compressibility coefficient of a molten globule core to be $60 \times 10^{-6}\,\mathrm{bar}^{-1}$, twice higher than that estimated for this native protein ($\sim 25 \times 10^{-6}\,\mathrm{bar}^{-1}$). It was suggested that a large hydration contribution results from an expansion of the hydrated outer surface of the molten globule and a loss of a portion of bulk water, which penetrated into the molten globule interior (internal hydration) [30].

4.3.2 Aggregation

4.3.2.1 Compressibility and Size of the Aggregates Aggregation is marked by a sharp decrease in the ultrasonic velocity, which coincides with an increase in attenuation. The decrease in the ultrasonic velocity for β-lactoglobulin at pH 7.5, observed at the aggregation stage (see Fig. 2 and Table 1), is about $-0.36\,\mathrm{m} \cdot \mathrm{s}^{-1}$. When corrected for the scattering contribution ($+0.1\,\mathrm{m} \cdot \mathrm{s}^{-1}$) this corresponds to a decrease in the concentration increment of the ultrasonic velocity of $-0.015\,\mathrm{cm}^3 \cdot \mathrm{g}^{-1}$ and an increase in the apparent adiabatic compressibility of $1.3 \times 10^{-6}\,\mathrm{bar}^{-1} \cdot \mathrm{cm}^3 \cdot \mathrm{g}^{-1}$. By performing the same calculations for other pH and heating rates studied, we found that, at the aggregation stage, the apparent compressibility changes by $(-1\text{ to }1.5) \times 10^{-6}\,\mathrm{bar}^{-1} \cdot \mathrm{cm}^3 \cdot \mathrm{g}^{-1}$ approximately. The overall changes in the apparent adiabatic compressibility result from two factors: the increase in the intrinsic compressibility of the protein interior and the contribution from a change in hydration. Therefore, the change in the intrinsic compressibility of protein due to combined denaturation and aggregation processes could be significantly different from the measured change in the apparent adiabatic compressibility. We explain the changes in the ultrasonic attenuation in terms of scattering of ultrasonic waves by the aggregates.

The overall increase in attenuation, and therefore the size of aggregates formed, varied significantly with pH (Fig. 2) and heating rates employed (Fig. 3). Using the set of thermophysical parameters described above, we calculated (PSize289 Software module) that the observed increase in attenuation corresponds to the size of aggregates of about 60 nm at pH 7.5 and between 100 and 300 nm at pH 6.0 (80 °C to 90 °C). These results are in good agreement with the average diameters (55 nm at 80 °C) of protein particles measured by us with light scattering (PCS) for pH 7.5. We could not perform the same comparison at pH 6.0, because of strong gelation in these samples resulting in artefacts in PCS measurements (effects of gel on diffusion of aggregates).

4.3.2.2 Effect of pH As it can be seen in Fig. 2 and Table 1, at pH 6.0 the aggregation stage occurred at a higher temperature than at pH 7.5. This shall be expected as pH 6.0 is closer to the protein isoelectric point (5.1) and therefore electrostatic repulsion between different protein molecules is lower at pH 6.0 compared with pH 7.5, thus making the native structure more resistant against unfolding. In addition, we shall expect that at pH 7.5 formation of disulfide-cross-links between aggregates (through thiol/disulfide exchange reactions) is more pronounced, as this pH is closer to the pKa of thiol group ($\sim$ 8.3). The observed larger size of the aggregates at pH 6 could also be explained by its closer value to the isoelectric point, which shall result in a higher electrostatic (dipole–dipole) attraction between different protein molecules.

It is interesting to note that the amplitude of the change in ultrasonic attenuation and velocity at the aggregation stage showed opposite trends as the pH of the protein solution was raised from 6.0 to 7.5. This could be explained by different scattering contributions to ultrasonic velocity, but may also suggest that aggregates formed at both values of pH have some differences in their intrinsic structures.

4.3.2.3 Effect of the Heating Rate It can be seen from Fig. 3 that the heating rate has a pronounced effect on the aggregation stage of the transition, i.e., major changes in ultrasonic parameters occur at lower temperatures for a slower heating rate, and the shape of attenuation profiles is also different. It is known that the thermal denaturation and aggregation of β-lactoglobulin is a multistage process, where the main stages occur with different rates [17,18], resulting in a shift of the temperature of aggregation towards high temperatures with faster temperature ramps. The increase of attenuation during the transition (Fig. 3) was lower at faster temperature ramps. This can be explained by a "quenching" of the quickly formed small protein nano-aggregates, which do not have enough time for further restructuring and flocculation into bigger aggregates, at high heating rates. The different effect of the ramp speed on the velocity and the attenuation temperature profiles can be explained by the fact that the velocity and attenuation represent different levels of the structural changes that occur. The velocity is mainly affected by changes of the compressibility of protein and its hydration shell during the transition to the molten globule state and formation of protein aggregates, while the attenuation is mainly affected by the formation and subsequent increase of the aggregate size. It is interesting to note that the increase in the heating rate causes a 'delay' of the attenuation curve relative to the velocity curve. At the highest rate, $1\,^{\circ}\mathrm{C}\cdot\mathrm{min}^{-1}$, the main drop in the ultrasonic velocity at the aggregation stage is completed at approximately 80 °C (Fig. 3), while at this temperature the

attenuation increase reached only one half of the total value. This again indicates that at high heating rates the formation of the intrinsic structure of the aggregates occurs much faster than the aggregation process overall, and that the aggregate growth at temperatures above 80 °C does not affect their intrinsic properties. A more detailed interpretation of the effects of the heating rate on the ultrasonic profiles of solutions of β-lactoglobulin will be provided in subsequent studies and discussed in conjunction with the kinetic (time) profiles of ultrasonic parameters at fixed temperatures.

4.3.3 Post-aggregation

This stage is marked by a linear decrease in ultrasonic velocity and a gradual increase in attenuation, followed by levelling off. The observed change in the slope in velocity may suggest that the "major" transition (formation of aggregates) is finished, and we observe temperature characteristics of the protein particles formed at the second stage of the process. A gradual increase in attenuation may suggest a slow increase of the particle size or an increase of viscous losses as a result of progressive cross-linking of protein aggregates.

Acknowledgments This project was supported by a 06RDTMFRC444 FIRM Grant from the Department of Agriculture and Food of Republic of Ireland and MASAF315 from SFI Ireland. We express our gratitude to Dr. Evgeny Kudryashov for his assistance in the experimental part of the work and discussions of the results.

References

1. M. Langton, A.M. Hermansson, Food Hydrocol. **5**, 523 (1992)
2. P.R. Kuhn, E.A. Foegeding, J. Agric. Food Chem. **39**, 1013 (1991)
3. R.H. Schmidt, V.S. Packard, H.A. Morris, J. Dairy Sci. **67**, 2723 (1984)
4. S. Ikeda, E.C.Y. Li-Chan, Food Hydrocol. **18**, 489 (2004)
5. S. Ikeda, V.J. Morris, Biomacromol. **3**, 382 (2002)
6. M.R.H. Krebs, G.L. Devlin, A.M. Donald, Biophys. J. **96**, 5013 (2009)
7. G.M. Kavanagh, A.H. Clark, S.B. Ross-Murphy, Int. J. Biol. Macromol. **28**, 41 (2000)
8. T. Lefevre, M. Subirade, Biopolymers **54**, 578 (2000)
9. E.H.C. Bromley, M.R.H. Krebs, A.M. Donald, Eur. Phys. J. E **21**, 145 (2006)
10. H.A. McKenzie, W.H. Sawyer, Nature **214**, 1101 (1967)
11. M. Verheul, J.S. Pedersen, S.P.F.M. Roefs, C.G. Kruif, Biopolymers **49**, 11 (1999)
12. X.L. Qi, C. Holt, D. Mcnulty, D.T. Clarke, Biochem. J. **324**, 341 (1997)
13. M.A.M. Hoffmann, P.J.J.M. Mil, J. Agric. Food Chem. **45**, 2942 (1997)
14. G.A. Manderson, L.K. Creamer, M.J. Hardman, J. Agric. Food Chem. **47**, 4557 (1999)
15. S. Iametti, B. de Gregori, G. Vecchio, F. Bonomi, Eur. J. Biochem. **237**, 106 (1996)
16. P. Busti, C.A. Gatti, N.J. Delorenzi, Food Res. Int. **38**, 543 (2005)
17. S.P.F.M. Roefs, C.G. de Kruif, Eur. J. Biochem. **226**, 883 (1994)
18. M.A.M. Hoffmann, J.C. van Miltenburg, J.P. van der Eerden, P.J.J.M. van Mil, C.G. de Kruif, J. Phys. Chem. B **101**, 6988 (1997)
19. M. Verheul, S. Roefs, C.G. de Kruif, J. Agric. Food Chem. **46**, 896 (1998)
20. W. Wang, Int. J. Pharm. **185**, 129 (1999)
21. V. Buckin, B. O'Driscoll, Lab Plus Int. **16**, 17 (2002)
22. V. Buckin, B. O'Driscoll, C. Smyth, Spectrosc. Eur. **15**, 20 (2003)
23. W.D. O'Brien Jr., F. Dunn, J. Phys.Chem. **76**, 528 (1972)
24. C.A. Miles, D. Shore, K.R. Langley, Ultrasonics **28**, 394 (1990)
25. W.G. Griffin, M.C.A. Griffin, J. Acoust. Soc. Am. **87**, 2541 (1990)

26. C.M. Bryant, D.J. McClements, Food Hydrocol. **13**, 429 (1999)
27. M. Corredig, M. Alexander, D.G. Dalgleish, Food Res. Int. **37**, 557 (2004)
28. D.P. Kharakoz, J. Phys. Chem. **95**, 5634 (1991)
29. D.P. Kharakoz, Biochemistry **36**, 10276 (1997)
30. D.P. Kharakoz, V.E. Bychkova, Biochemistry **36**, 1882 (1997)
31. T.V. Chalikian, V.S. Gindikin, K.J. Breslauer, J. Mol. Biol. **250**, 291 (1995)
32. T.V. Chalikian, J. Völker, D. Anafi, K.J. Breslauer, J. Mol. Biol. **274**, 237 (1997)
33. T.V. Chalikian, M. Totrov, R. Abagyan, K.J. Breslauer, J. Mol. Biol. **260**, 588 (1996)
34. N. Taulier, T.V. Chalikian, J. Mol. Biol. **314**, 873 (2001)
35. N. Taulier, T.V. Chalikian, Biochim. Biophys. Acta **1595**, 48 (2002)
36. C. Smyth, K. Dawson, V. Buckin, Prog. Colloid Polym. Sci. **115**, 287 (1999)
37. L. Lehmann, V. Buckin, J. Dairy Sci. **88**, 3121 (2005)
38. C. Smyth, E. Kudryashov, V. Buckin, Colloids Surf. A **183**, 517 (2001)
39. C. Dwyer, L. Donnelly, V. Buckin, J. Dairy Res. **72**, 302 (2005)
40. K. Bell, H.A. McKenzie, Biochim. Biophys. Acta **147**, 109 (1967)
41. V.A. del Grosso, C.W. Mader, J. Acoust. Soc. Am. **52**, 1442 (1972)
42. P.C. Waterman, R. Truell, J. Math. Phys. **2**, 512 (1961)
43. J.R. Allegra, S.A. Hawley, J. Acoust. Soc. Am. **51**, 1545 (1972)
44. M.J.V. Povey, *Ultrasonic Techniques for Fluids Characterization* (Academic Press, London, 1997)
45. Y. Choi, M.R. Okos, in *Food Engineering and Process Applications*, ed. by L. Maguer, P. Jelen Hinz (Elsevier, London, 1986), p. 93
46. J.M. Simonson, J. Chem. Thermodyn. **26**, 345 (1994)
47. C.-T.A. Chen, J. Chem. Eng. Data **27**, 356 (1982)
48. S. Likke, L.A. Bromley, J. Chem. Eng. Data **18**, 189 (1973)
49. H. Ozbek, S.L. Phillips, J. Chem. Eng. Data **25**, 263 (1980)
50. F.J. Millero, F. Vinokurova, M. Fernandez, J.P. Hershey, J. Solution Chem. **16**, 269 (1987)
51. R.J. Urick, J. Appl. Phys. **18**, 983 (1947)
52. V. Buckin, Biophys. Chem. **29**, 283 (1988)
53. H. Durchschlag, in *Thermodynamic Data for Biochemistry and Biotechnology*, ed. by H.-J Hinz (Springer-Verlag, Berlin, Heidelberg, 1986), chap. 3
54. S. Hickey, M.J. Lawrence, S.A. Hagan, V. Buckin, Langmuir **22**, 5575 (2006)
55. J. Stuehr, E. Yeager, in *Physical Acoustics*, ed. by W.P. Mason (Academic Press, New York, Heidelberg, 1965), p. 351
56. A.P. Sarvazyan, P. Hemmes, Biopolymers **18**, 3015 (1979)
57. A.P. Sarvazyan, D.P. Kharakoz, P. Hemmes, J. Phys. Chem. **83**, 1796 (1979)
58. M. Hussey, P.D. Edmonds, J. Phys. Chem. **75**, 4012 (1971)
59. K.C. Cho, W.P. Leung, H.Y. Mok, C.L. Choy, Biochim. Biophys. Acta **830**, 36 (1985)
60. P.K. Choi, J.-R. Bae, K. Takagi, J. Acoust. Soc. Am. **87**, 874 (1990)
61. T.V. Chalikian, V.S. Gindikin, K.J. Breslauer, FASEB J. **10**, 164 (1996)
62. P.S. Epstein, R.R. Carhart, J. Acoust. Soc. Am. **25**, 553 (1953)
63. B. Nolting, S.G. Sligar, Biochemistry **32**, 12319 (1993)
64. Y. Tamura, K. Gekko, Biochemistry **34**, 1878 (1995)
65. T. Kamiyama, K. Gekko, Chem. Lett. **26**, 1063 (1997)